Multi-Instrument Data Analysis System (MIDAS) Imaging of the Ionosphere

Report for the United States Air Force European Office of Aerospace Research and Development

February 2002

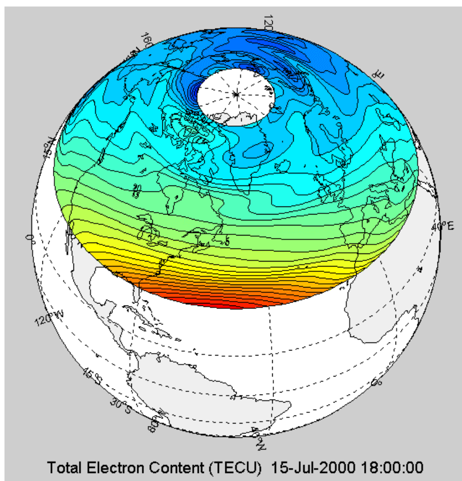

Scientific investigators: Dr C N Mitchell and Prof P S Cannon
Research officer: Dr P S J Spencer

Contact details: Dr C. N. Mitchell,
Department of Electrical and Electronic Engineering,
University of Bath, Bath BA2 7AY, UK.
Tel: +44 1225 826610
Email C.N.Mitchell@bath.ac.uk

UNIVERSITY OF BATH

Report Documentation Page

Form Approved
OMB No. 0704-0188

1. REPORT DATE **11 MAR 2002**	2. REPORT TYPE **N/A**	3. DATES COVERED **-**

4. TITLE AND SUBTITLE **Multi-Instrument Data Analysis System (MIDAS) Imaging of the Ionosphere**	5a. CONTRACT NUMBER 5b. GRANT NUMBER 5c. PROGRAM ELEMENT NUMBER
6. AUTHOR(S)	5d. PROJECT NUMBER 5e. TASK NUMBER 5f. WORK UNIT NUMBER
7. PERFORMING ORGANIZATION NAME(S) AND ADDRESS(ES) **University of Bath Univ. of Bath Bath BA2 7AY United Kingdom**	8. PERFORMING ORGANIZATION REPORT NUMBER
9. SPONSORING/MONITORING AGENCY NAME(S) AND ADDRESS(ES)	10. SPONSOR/MONITOR'S ACRONYM(S) 11. SPONSOR/MONITOR'S REPORT NUMBER(S)

12. DISTRIBUTION/AVAILABILITY STATEMENT
Approved for public release, distribution unlimited

13. SUPPLEMENTARY NOTES
The original document contains color images.

14. ABSTRACT

15. SUBJECT TERMS

16. SECURITY CLASSIFICATION OF:			17. LIMITATION OF ABSTRACT	18. NUMBER OF PAGES	19a. NAME OF RESPONSIBLE PERSON
a. REPORT **unclassified**	b. ABSTRACT **unclassified**	c. THIS PAGE **unclassified**	**UU**	**30**	

Standard Form 298 (Rev. 8-98)
Prescribed by ANSI Std Z39-18

Summary

A new technique has been developed to reveal the temporal and spatial distribution of ionization in the ionosphere and plasmasphere.. The technique uses freely-available GPS satellite data over the continents of the Northern Hemisphere to produce fully four-dimensional ‘movies’ of the ionization distribution. In this report a quantitative, large-scale study has been undertaken to evaluate the technique over the USA. The research focuses on two periods. The first is a geomagnetically quiet time just past solar minimum during February 1997. The second is during current solar maximum around the extreme ionospheric storm of July 2000.

Two different types of imaging have been assessed – firstly with just ground-based GPS data and then with radio occultation (GPS-to-LEO satellite) data in the inversion. Imaging with ground-based GPS data alone can provide limited but useful information about the vertical profiles of ionization and this is demonstrated during the July 2000 storm. Comparisons with ionosonde observations indicate that GPS/MET radio occultation data improve the determination of the peak electron concentration by providing more information about the vertical profile of ionization. Such satellite data is particularly important in improving the image quality at the edge of the ground-based coverage, over the oceans. Recommendations are made for future research to evaluate the benefit of including data from ionosondes and Langmuir probes into the inversion.

Contents

.

1 Introduction

Large-scale mapping of electron concentration and total electron content (TEC) can be performed using a variety of different methods. Models based on long-term, statistical records can provide useful indications of time-averaged conditions, but are generally not suitable for accurate representations of the ionosphere at any instant. This is because the short-term variability of the ionosphere regularly causes the ionospheric morphology to differ from time-averaged conditions. Irregular features such as travelling ionospheric disturbances (TIDs) in the day and the main trough and auroral structures at night are difficult to predict without the operation of real-time sensors. However, incorporating a large number of varying spatial and temporal observations into a model is not a straightforward procedure. In this report we test one possible solution to combining measurements, based on extensions of the mathematical ideas used in tomographic imaging.

A new inversion program (MIDAS[1]) used here extends tomography into four-dimensional spatial-temporal mapping. The great advantage is that all observations can be combined simultaneously in a single inversion with the minimum of a priori assumptions about the form of the ionospheric electron-concentration distribution. Tomographic techniques have been applied to the problem of ionospheric imaging since 1986 (Austin et al. 1986), where TRANSIT satellite transmissions, from an orbital altitude of approximately 1100 km, have been utilized to make two-dimensional cross-sections of the ionosphere in a latitude-height quasi-plane. However, since the original proposal to use TRANSIT satellites many other instruments have come on line, providing an inhomogeneous distribution of ionospheric information. At present, the most numerous and easily accessible data come from the International GPS network of ground-based GPS receivers. This coverage of data is now sufficiently extensive over the USA and Europe to allow imaging over these continental regions.

Another important new ionospheric measurement comes from GPS to Low-Earth-Orbit (LEO) satellites. This technique, known as radio-occultation, uses receivers located on LEOs to monitor phase changes of GPS signals. Hajj et al. (1994) suggested using the satellite-to-satellite transmission of GPS to LEO measurements in a tomographic framework to provide the so-called ‘missing horizontal rays’ and improve the vertical resolution. In addition, LEOs provide measurements over the oceans and into remote polar caps, thus enabling the ionosphere to be studied on a truly global-scale. Past and current LEO missions include GPS/MET and more recently OERSTED, SAC-C, IOX and CHAMP. There are several new radio-occultation satellites planned for launch over the next ten years, notably a constellation of LEOs known as COSMIC. In this report particular attention is given to demonstrating the advantage of including radio occultation data in the inversion.

This report contains case-study evaluations of the MIDAS technique, applied to the ionosphere over the USA. Section 2 provides a basic introduction to imaging of the

[1] Mult-instrument Data Analysis System © University of Bath

ionosphere and the theory of the MIDAS inversion method. In Section 3 examples are shown of the inversion of simulated data for a two-dimensional geometry, demonstrating that for TEC evaluation a tomographic inversion is more accurate than a thin-shell calibration. In Section 4 the full four-dimensional inversion is performed on experimental data over the USA. A case study is shown for a period in 1997 at the end of the GPS/MET mission. This period was chosen because both ground- and space-based GPS data were available simultaneously. The advantage in using the radio occultation data (GPS/MET) in the inversion is evaluated by comparisons with independent co-located ionosonde measurements. In Section 4 the inversion technique is tested for the period of the extreme storm of July 2000. Again, ionosonde data is used for comparison. Finally, conclusions and recommendations for future directions of the work are in Section 5.

2 Tomographic Imaging

Tomography involves imaging a parameter in two dimensions, using measurements taken along a large number of intersecting paths. Each separate view of the object along the different paths provides information about that path integral and is known as a projection. These one-dimensional projections are combined using a reconstruction algorithm to obtain a tomographic image of the parameter. To facilitate an understanding of tomography it is instructive to consider the following simple problem. A square grid (Figure 1) contains four unknown numbers. Each element of the grid has sides of unit length and is known as a pixel. The summation of the numbers along particular lines (projections or ray paths) passing through the pixels are measured. These projections constitute a set of tomographic observations.

The inversion problem is to find the numbers in the grid using only the information gained from the projections. For example, if each of the numbers within the grid was equal to one, then the summation directly along any row or column would be two. For projections which cross the grid at an oblique angle it becomes necessary to utilize the amount by which each raypath crosses each grid element. Hence the summation along the diagonal of the grid would be $\sqrt{2}+\sqrt{2}$. By simple geometry the summation of numbers along any arbitrary raypath can be calculated (for example for projection i_2, entering the grid at an angle of 22.5° to the horizontal). For this illustrated problem the measurement set would contain the information that measurement i_1=2, measurement i_2=2.4 and measurement i_3=2.8.

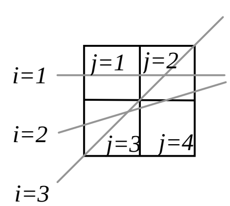

Figure 1. Two-by-two grid with indexed projections, i, and pixels, j.

Using the locations of the start and end point of each projection (from the locations of the transmitter and receiver), and the tomographic measurements the problem can therefore be formulated as follows. Each projections is given an index (*i*) and each pixel an index (*j*). The measurements are given the symbol y_i and the known length of each projection through each pixel the symbol A_{ij}. The unknown number in each pixel is designated x_j. For the first raypath this would form the equation,

$$y_1 = A_{11}x_1 + A_{12}x_2 \qquad [1]$$

etc.

The task is thus to find the value of each unknown, x_j, given the set of measurements, y_i. The resulting set of simultaneous equations can be solved using standard matrix inversion theory. It should be noted that for a unique mathematical solution sufficient measurements must be made. Clearly if only one measurement was taken, Equation 1 could be satisfied with many different solutions for x_1 and x_2. Additionally, the measurement set should cross each of the pixels and project over the full range of viewing angles (Figure 2). In many practical applications of tomography it is not possible to satisfy these conditions and it becomes necessary to constrain the solution with other information, such as physical models or a-priori knowledge.

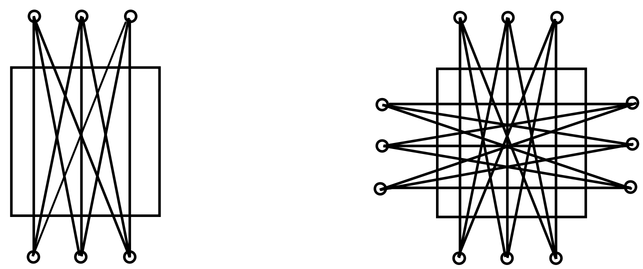

Figure 2. Diagrams illustrating the geometrical biases in projections resulting in underdetermined (left) and fully determined (right) inversions.

2.1 Ionospheric Imaging using MIDAS

This Section describes the MIDAS technique for imaging the ionosphere. Figure 3 illustrates the complicated geometry that is created by multiple satellite-to-receiver and satellite-to-satellite measurements. In order to overcome the requirement to specify the plane of the image in 2-D (as is approximated for in NNSS tomography) a new technique has been developed. The MIDAS algorithm was designed, written and tested at the University of Bath under an EPSRC contract (C.N. Mitchell and P.A. Watson, June 2000-Aug 2001). This analysis algorithm can use dual-frequency observations from the GPS satellites to produce four-dimensional images of electron concentration over very large geographical regions (potentially globally). MIDAS also has the facility to incorporate other ionospheric measurements, such as electron-concentration profiles from inverted ionograms or in-situ measurements of ionization concentration from satellites in low-earth-orbit.

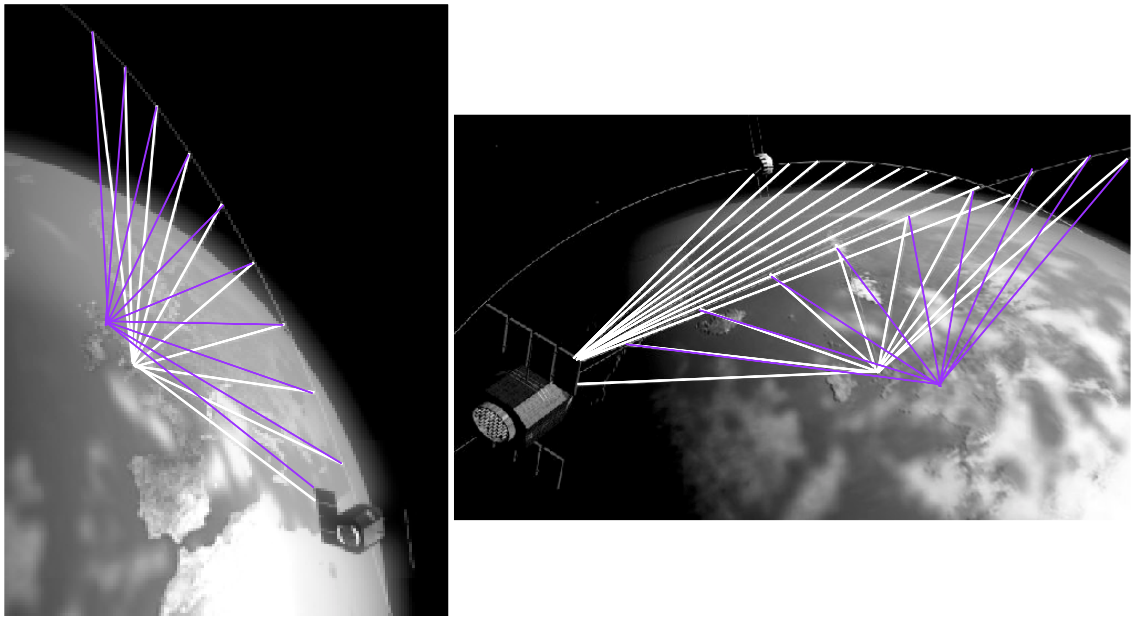

Figure 3. Diagrams illustrating the geometrical biases involved in the special case of conventional TRANSIT-to-ground (left) and the more general GPS to LEO and LEO-to-ground (right). The orientations of the projections from radio occultation complement those from satellite-to-ground, but do not provide a perfect geometrical coverage for a fully determined tomographic inversion.

Ordinary ionospheric tomography uses a two-dimensional inversion from a single polar-orbiting satellite. During the over-fly of this satellite (typically taking 20 minutes) the ionization distribution is assumed to be stationary. It had been thought that GPS satellites could not be used for ionospheric imaging because the satellite orbits are high and so the transit time is many hours – too long to image a moving ionosphere. However, multiple GPS satellites are in view at any time and this work exploits this fact to allow a fully four-dimensional determination of the ionization distribution with a time sample of 30 seconds – i.e. the time evolution of three-dimensional structures can be studied. The inversion thus results in a 3-D ‘movie’ rather than the static 2D slice produced by a tomographic inversion. Individual frames of the ‘movie’ can then be used for spatial studies. Studies of the temporal changes in the ionosphere can be made with successive frames.

Previous techniques involved the independent analysis of either (i) satellite-to-satellite radio-occultation observations or (ii) satellite-to-ground GPS. However, these latter two methods are inherently complementary in their strengths and weaknesses, which are:

- 4-D inversions of satellite-to-ground GPS observations demonstrate a good horizontal resolution capable of imaging the main trough but have limited vertical resolution.
- Satellite-to-satellite radio-occultation observations demonstrate good vertical resolution but have poor horizontal resolution.

Consequently, the simultaneous inversion of both satellite-to-ground and satellite-to-satellite GPS data in a single algorithm provides a greatly improved geometry in comparison to that found when using either data set independently. Table 1 summarizes the different types of measurements that can be put into the MIDAS inversion and details their strengths.

Measurement	**Linear inversion in MIDAS?**	**Advantages**
Satellite-to- ground	Yes	Data easily available Horizontal resolution
Satellite-to- satellite	Yes	Vertical resolution Global coverage including oceans and poles Topside and plasmasphere
Sea-reflecting radar	Yes	Oceans covered Horizontal gradients
Ionosonde	Only after real-height inversion	Vertical resolution
***In situ* measurement**	Yes	Non-integrated (anchor-point for the inversion)

Table 1. Diagram showing the types of instrument, inversion and advantages of the measurement type for the ionospheric MIDAS inversion.

The software implements a linear inversion algorithm to solve for the distribution of electron concentration in the ionosphere. Figure 4 gives an overview of analysis of different types of measurement used in the software. Figure 5 shows the configurable options for different types of inversion. These two diagrams can be used to aid in the choice of inversion for different types of data. For example:

1. If a wide-area 3-D map of electron concentration were needed over Europe then ground and space-based GPS and inverted ionosonde data could be used in a 4-D inversion and individual frames of the resulting ‘movie’ could be plotted to show the values of electron concentration at a given time in each voxel.

2. If a wide-area 3-D map of electron concentration were needed over the Atlantic then ground-based GPS from Europe and USA could be inverted with radio occultation

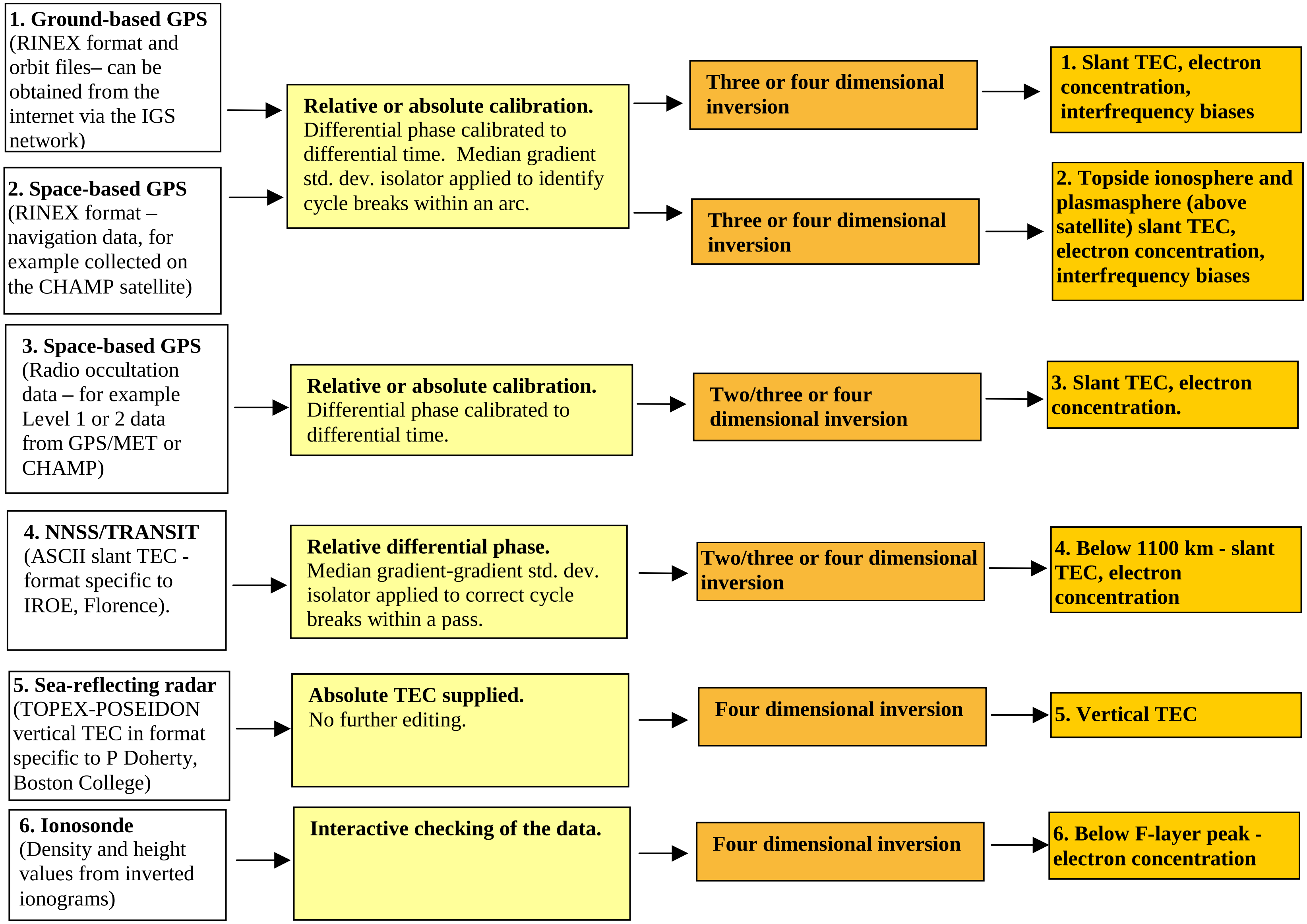

Figure 4. Diagram showing the types of raw data, processing, recommended inversion and output strengths for the ionospheric MIDAS inversion. All four-dimensional inversions use ground-based GPS, with other data sources if available.

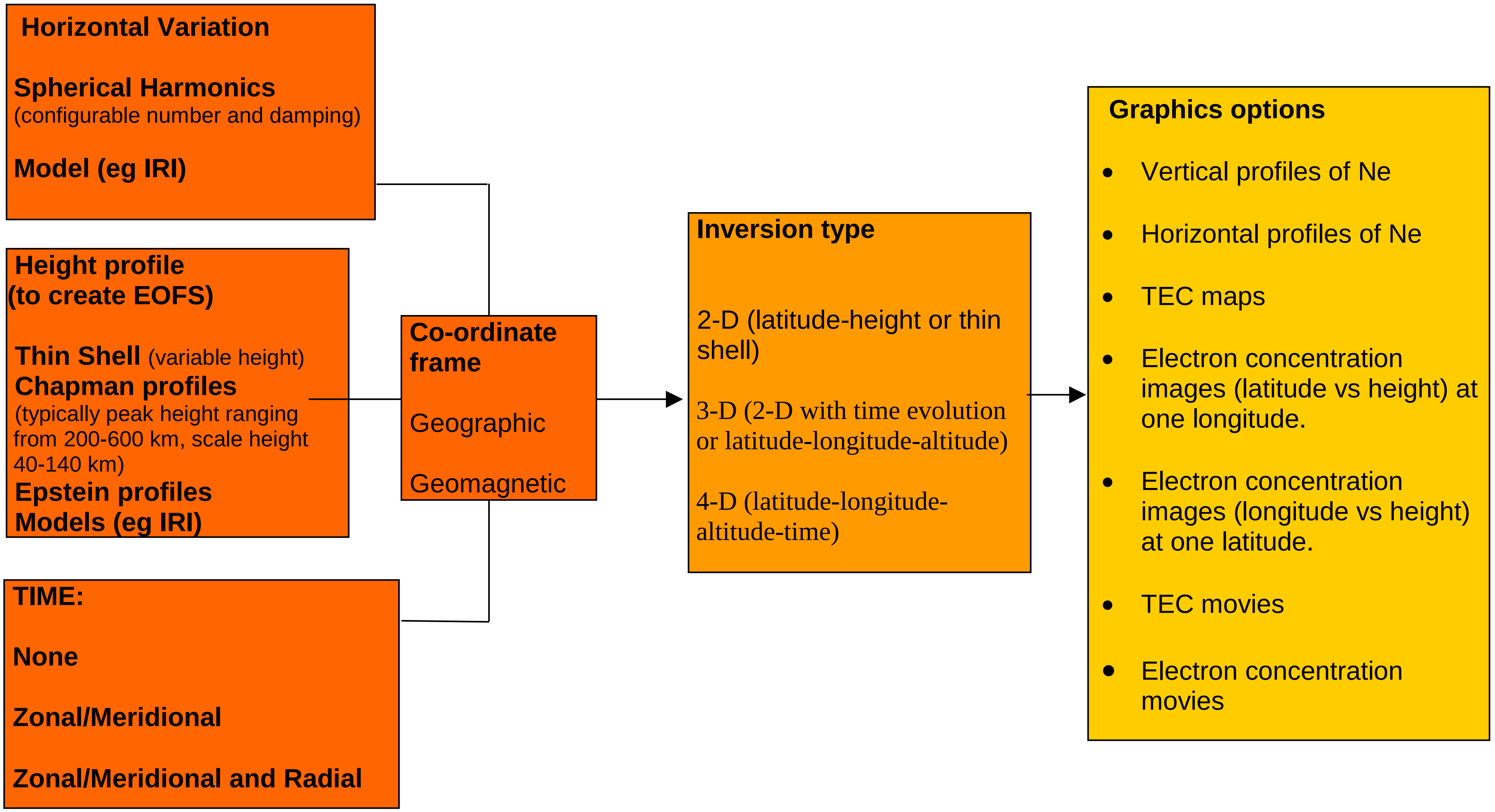

Figure 5. Diagram showing the configurable options set at the command interface of the MIDAS software.

data and sea-reflecting radar over the oceans. If the ocean data were sparse then a model (rather than spherical harmonics) could be used to form the basis functions.

Dual frequency radio signals that propagate through the ionosphere are subject to a differential phase change due to the dispersive nature of the medium. Provided lock is maintained on both frequencies the change in the differential phase shift is directly proportional to the change in integrated total electron content (TEC) between the transmitter and receiver. In the case of GPS, since the actual satellite-to-receiver ionospheric path is constantly changing, this change in TEC is a composite of spatial and temporal effects. GPS satellites also provide P-code observations (time delay) enabling an estimate of the absolute TEC along the ray path. However, these time-delay estimates are subject to transmitter and receiver clock biases and to the effects of multi-path. The current implementation of MIDAS allows for both types of observations (differential phase and differential time) to be included in the inversion.

The first stage in the inversion problem is to set up a grid of three-dimensional voxels in a spherical volume and compute the elemental contributions from each of the satellite-to-receiver ray path integrals. Defining the electron concentration within each voxel as x, the problem may be expressed as,

$$Ax = b \tag{2}$$

where A is a sparse matrix of the path lengths within each voxel and b are the observed line integrals (TEC). The matrix A is highly singular and incorporates no prior information as to the likely solution. To overcome this difficulty a mapping matrix, M, is used to transform the problem to one for which the unknowns are a set of appropriately selected ortho-normal basis functions. This is expressed mathematically as,

$$AMX = b \tag{3}$$

where the matrix M defines the mapping from a voxel based representation to an ortho-normal representation of the reconstruction volume. Since the ray-paths integrals derived from phase are subject to an unknown cycle offset adjacent rows of the matrices AM and b are differenced so as to negate the effect of this on the solution. The unknowns, X, now represent the relative contribution of the basis functions where,

$$X = (AM)^{-1} b \tag{4}$$

Applying singular value decomposition to the matrix AM returns two orthogonal matrices U and V and a diagonal matrix of singular values, w. The solution to the inverse problem is then given by

$$X = (V.(diag(1/w).U^T).b \tag{5}$$

where the reciprocal of the terms in *w* that are sufficiently small, typically 10^{-7} of the dominant singular weight, are zeroed. Finally, the electron densities within each voxel are recovered using,

$$x = TX \qquad [6]$$

The choice of ortho-normal basis functions is critical in the determination of the final solution. For this report the basis functions were generated using a spherical harmonic expansion to represent the horizontal variation and empirical ortho-normal functions (EOFs) for the radial variation in electron concentration. Each basis function in the series may be optionally allowed freedom to evolve linearly in time. The functional form of the basis function solution is given by,

$$P_l^m(\cos(\theta)).\left[(X_{2i} + \frac{\partial X_{2i}}{\partial t}t)\sin(m\phi) + (X_{2i+1} + \frac{\partial X_{2i+1}}{\partial t}t)\cos(m\phi)\right].E_n(r) \qquad [7]$$

where P represents the series of Legendre polynomials in latitude, θ, φ is the longitude and E represents the empirical ortho-normal functions in radius, r.

3 Two-Dimensional Inversions using Simulated TEC

Extensive studies into the application of two-dimensional tomographic techniques to ionospheric imaging have been carried out for a number of years. The two-dimensional geometry arises from the fact that TRANSIT satellites are polar orbiting and as such a line of receivers located along a meridian almost form an intersecting geometry that lies in a two-dimensional plane. The MIDAS inversion can be run in a mode similar to that applied to the 2D tomographic problem by Fremouw et al. (1992). It is instructive to consider the two-dimensional case in order to gain an understanding of the problems involved in higher dimensional inversions.

Figure 6 shows an example of the inversion of simulated TEC observations (created using the modeling feature within MIDAS) from an ionosphere that included a trough and a step in the peak-height. Model data was generated for six ground-based receivers located at latitudes from 35^o to 60^o at 5^o intervals. Data obtained from each model receiver was assumed to be subject to an unknown cycle-offset and consequently the method of ray differencing was used. The basis functions used for this inversion consisted of 60 Legendre polynomials representing the latitudinal variation and only 2 empirical ortho-normal functions (EOFs) in the radial direction. The EOFs, shown in Figure 7, were generated using singular value decomposition (SVD) from a limited range of Chapman profiles with peak heights ranging from 250km to 350km.

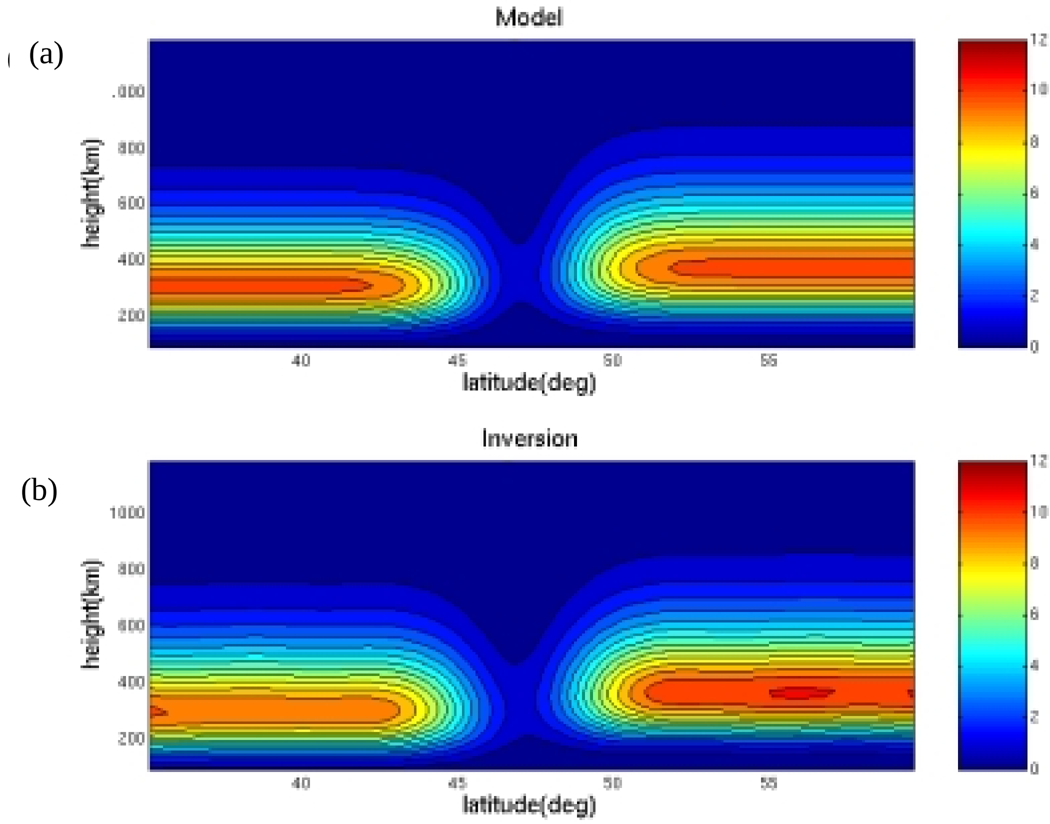

Figure 6. Model electron concentration cross-section (a) and 2D inversion (b) (electron concentration in units of $10^{11}m^{-3}$)

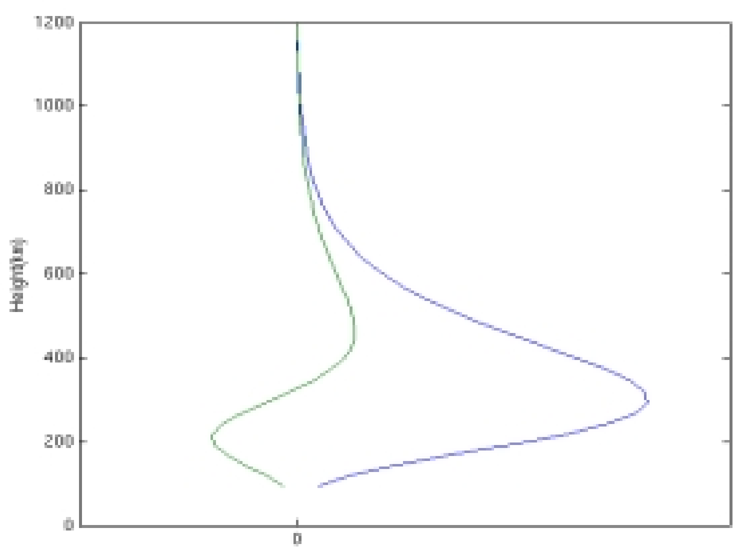

Figure 7. Empirical ortho-normal functions used to describe the radial electron concentration variation.

Figure 8 presents the latitudinal variation in vertical total electron content (TEC) obtained from the model and from a number of inversions. The black curve shows the variation of vertical TEC with latitude for the input model data as presented in Figure 6a. The other three curves show the results for inversions for which the representation of the distribution of ionization in the radial direction was varied. In all three cases a grid resolution of 0.25^o in latitude was used together with 60 Legendre polynomials. It is clear that the thin-shell approximation (all ionization at one altitude), shown in magenta, is a very poor representation of the ionosphere in the presence of significant latitudinal gradients. A single EOF solution, given by the red curve, is a significant improvement, reproducing the trough location and shape very accurately. Finally the two EOF solution corresponding to Figure 6b, and shown in blue, provides most accurate TEC estimates with errors typically 5% or less. It must be stressed that the improvement obtained in going from one EOF to two is small. This is equivalent to the statement that the amount of information in the observations from ground-based instrumentation concerning the vertical profile is subtle. With ground-based TEC observations alone it is often not possible to obtain stable solutions with more than two degrees of freedom for the basis functions in the radial direction. Nevertheless, for the calculation of vertical TEC, the major improvement is between thin-shell and full inversion.

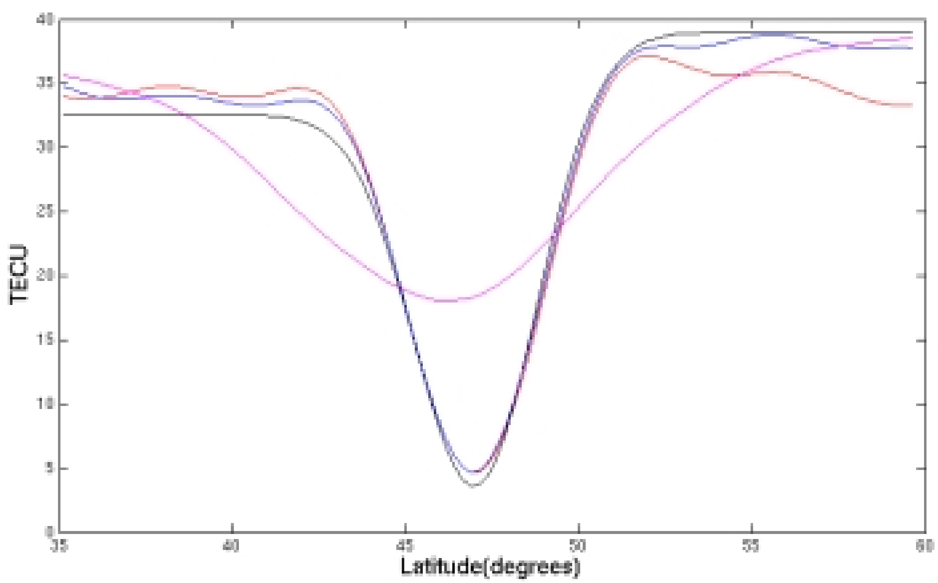

Figure 8. Comparison of vertical TEC from model (black) and inversions using; 450km Shell (magenta), one EOF (red), two EOFs (blue)

4 GPS/MET Case Study: 20th to 23rd February 1997

In this Section results are presented from a case study of the ionosphere over the USA during February 1997. The geomagnetic conditions were fairly quiet, with Kp values between 0 and 4. This time period was chosen due to the availability of GPS/MET data towards the end of the satellite's life, when the ground-based IGS data were becoming more extensive. Figure 9 shows the distribution of IGS ground-based receivers used in the study.

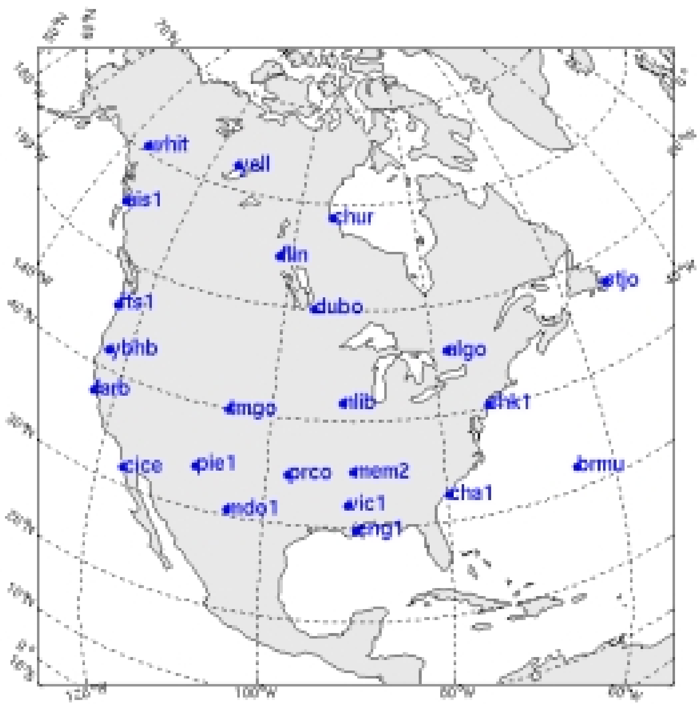

Figure 9. Plot of IGS receivers used for the 1997 case study.

Ground-based GPS data from the IGS network were used in four-dimensional inversions. Each inversion was set to run using a one-hour data set and hence over the four days there were 96 one-hour inversions. The IGS data are available at a 30-second sample rate and these were under-sampled by a factor of four to reduce the computational time (typically taking ten minutes to produce a one-hour movie of the ionosphere). A preliminary set of inversions was generated using ground-based phase data with 40 Legendre polynomials, two longitudinal harmonics and two EOFs. The inversions were then used to estimate the least-squares values of satellite and receiver inter-frequency biases over the four-day period of study. The bias estimates obtained are shown in Figure 10. A red dot indicates a bias estimate; a green dot indicates no estimate for that particular inversion. These averaged estimates of bias (blue lines) were then used to improve the time-delay (P-code) data for subsequent inversions, so that the differential phase could be calibrated to the differential time. It is clear from this plot that the independent bias estimates were consistent on an hour-by-hour basis. Using these biases the phase observations were calibrated and another set of inversions was computed with

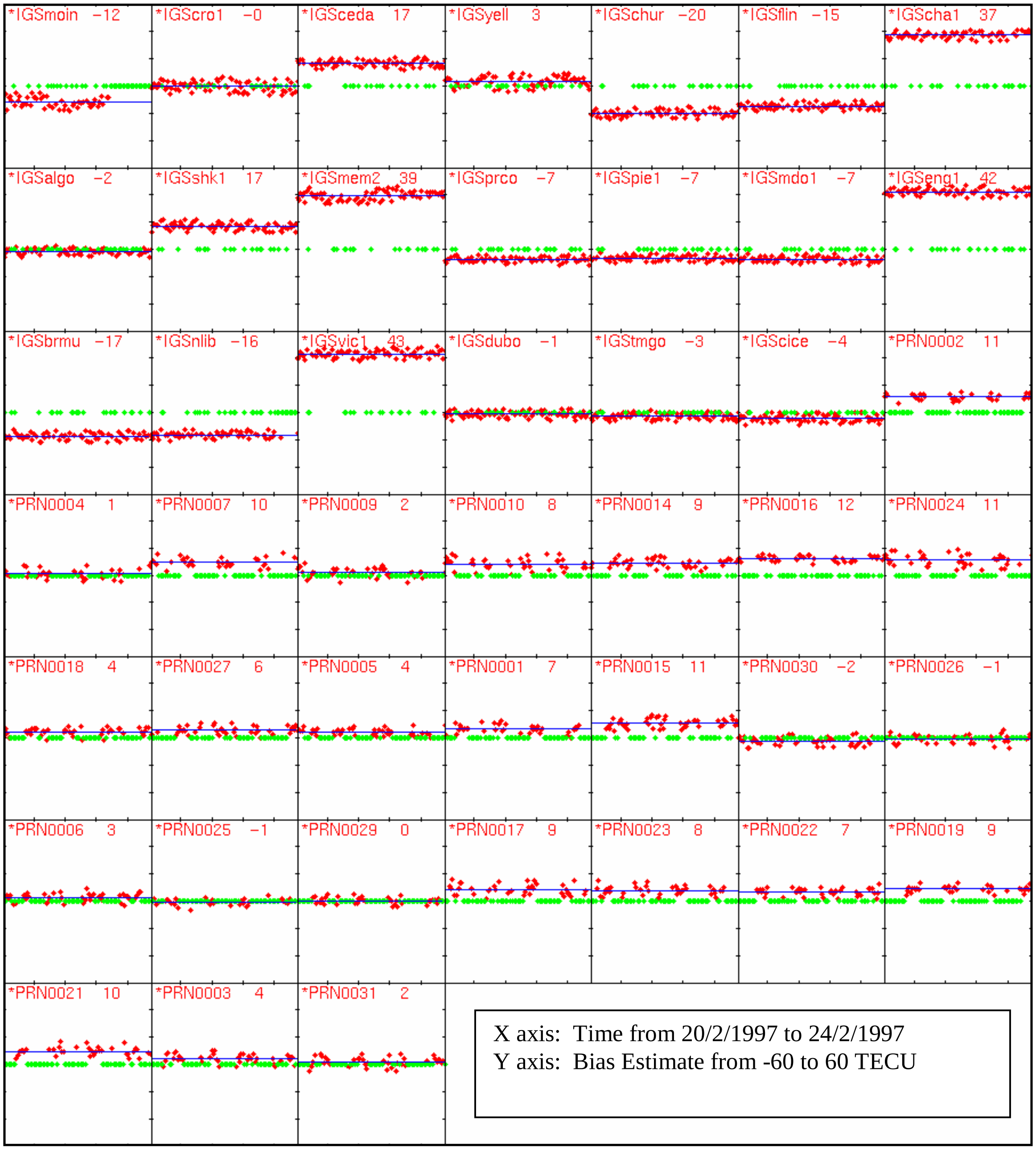

Figure 10. Independent satellite and receiver bias estimates (TECU) obtained from each one-hour inversion. Red points show bias estimate, green points indicate no solution.

the same set of basis functions.

In a second stage, inversions were computed from combined ground- and space-based GPS observations for each hour of data when radio-occultations occurred over the US mainland. For these inversions five EOFs were used, since the LEO data contains more information about the vertical profile. It should be noted that no selection of these passes was made to remove results where the occultation geometry was poor. The aim here is to show that any GPS-to-LEO satellite ionospheric observations can improve the accuracy of the inversion in determination of the vertical electron-concentration profile. In the LEO case only phase measurements, rather than time delay, were utilized.

Ionosonde observations of foF2 at four locations in the USA were converted to peak electron concentration. The voxels of electron concentration from the MIDAS inversions at the same latitude and longitude and time as the ionosonde sounding were scanned to obtain the peak electron concentration in that column (peak F-layer density). These values were then compared to the ionosonde data. The peak densities obtained from these ground-based only inversions (pink) and the corresponding ionosonde values (blue) are shown in Figure 11. It can be seen that the comparison is good for the northerly ionosondes and degrades towards the south. This is probably affected by the distribution of GPS receivers (Figure 9) since the most southerly ionosonde, at 30.4^{o}N, is on the edge of the receiver network. Differences are pronounced during the nighttime, when diffusion in the ionosphere results in larger scale heights and higher peak heights. It is likely that the two EOFs here, while representing the profile adequately during the day, are insufficient to accommodate this increased scale height at night. Since the TEC values are correct, the result of an underestimate of the scale-height is an over-estimate of the peak electron concentration. This effect is most apparent to the edge of the network, where information is most directionally biased and sparse. In these regions the vertical profiles will effectively default towards the first EOF.

Figure 12 shows the ionosonde data compared to the MIDAS inversions using both radio occultation and ground-based GPS data. Points have only been shown where the GPS/MET satellite orbit passed over mainland USA. The results indicate a general improvement in the comparison. Importantly, the MIDAS peak electron concentrations during the nighttime compare very favorably with the ionosonde values. The radio occultation data allowed an increase in the number of EOFs representing the vertical profile, and consequently the larger scale-heights and lower peak densities have been accommodated. A second point to note is that the improvement in the results was significant at the edge of the image region. This indicates that the radio occultation improves the imaging accuracy over data-sparse regions such as oceans.

Examples of cross-sections through four images at a longitude of 98ºW obtained on the 21st February (Day 52) are shown in Figure 13. The daytime peak height is typically 270 km, whereas the nighttime one is higher between 300 km and 400 km. The scale-heights are also larger at night, confirming the improvements shown by the inclusion of the GPS/MET data.

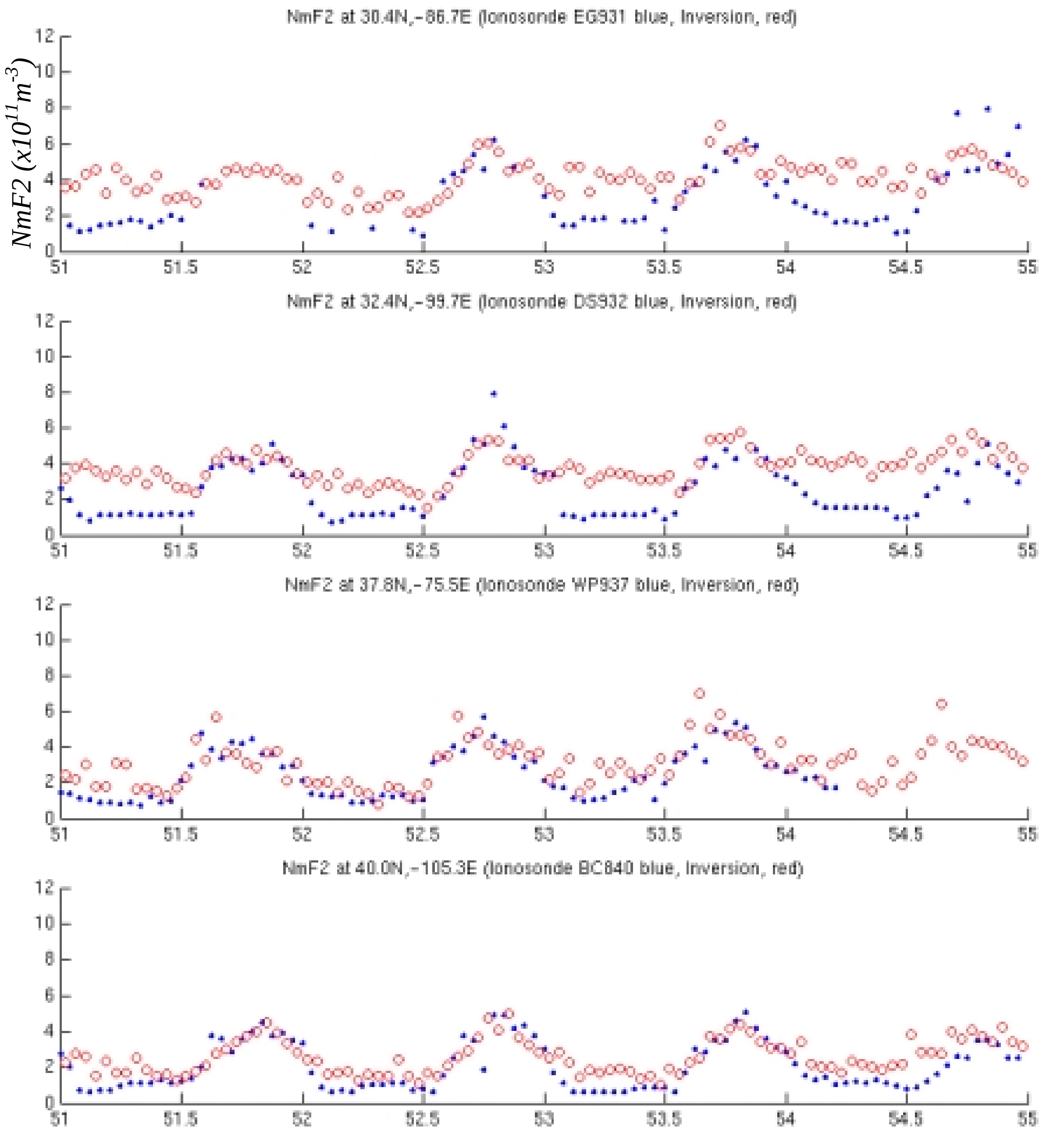

Figure 11. Comparison of NmF2 ($x10^{11}$ m^{-3}) from ionosondes and inversions using ground and space-based GPS data

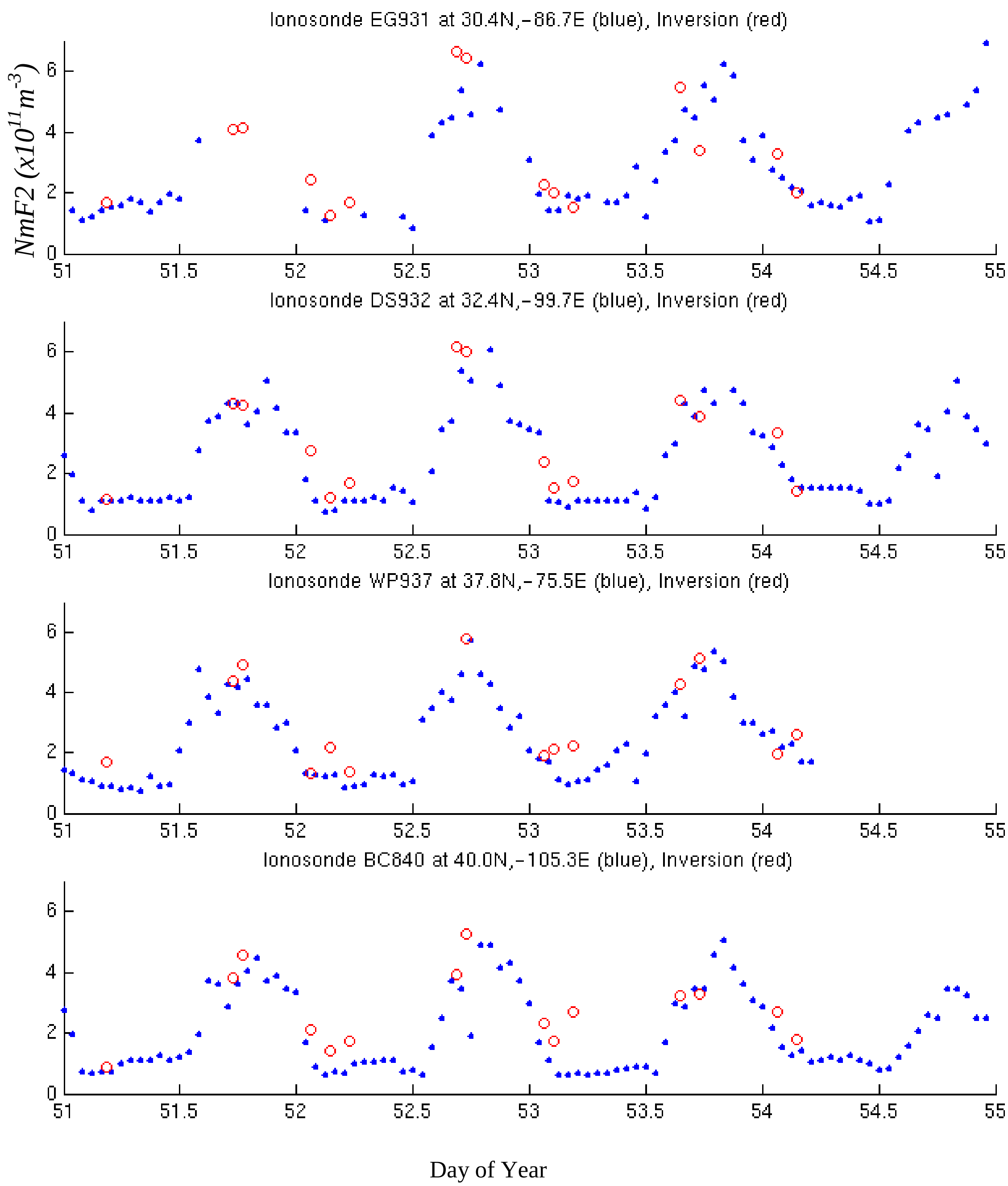

Figure 12. Comparison of NmF2 ($x10^{11}$ m^{-3}) from ionosondes and inversions using ground-based GPS data

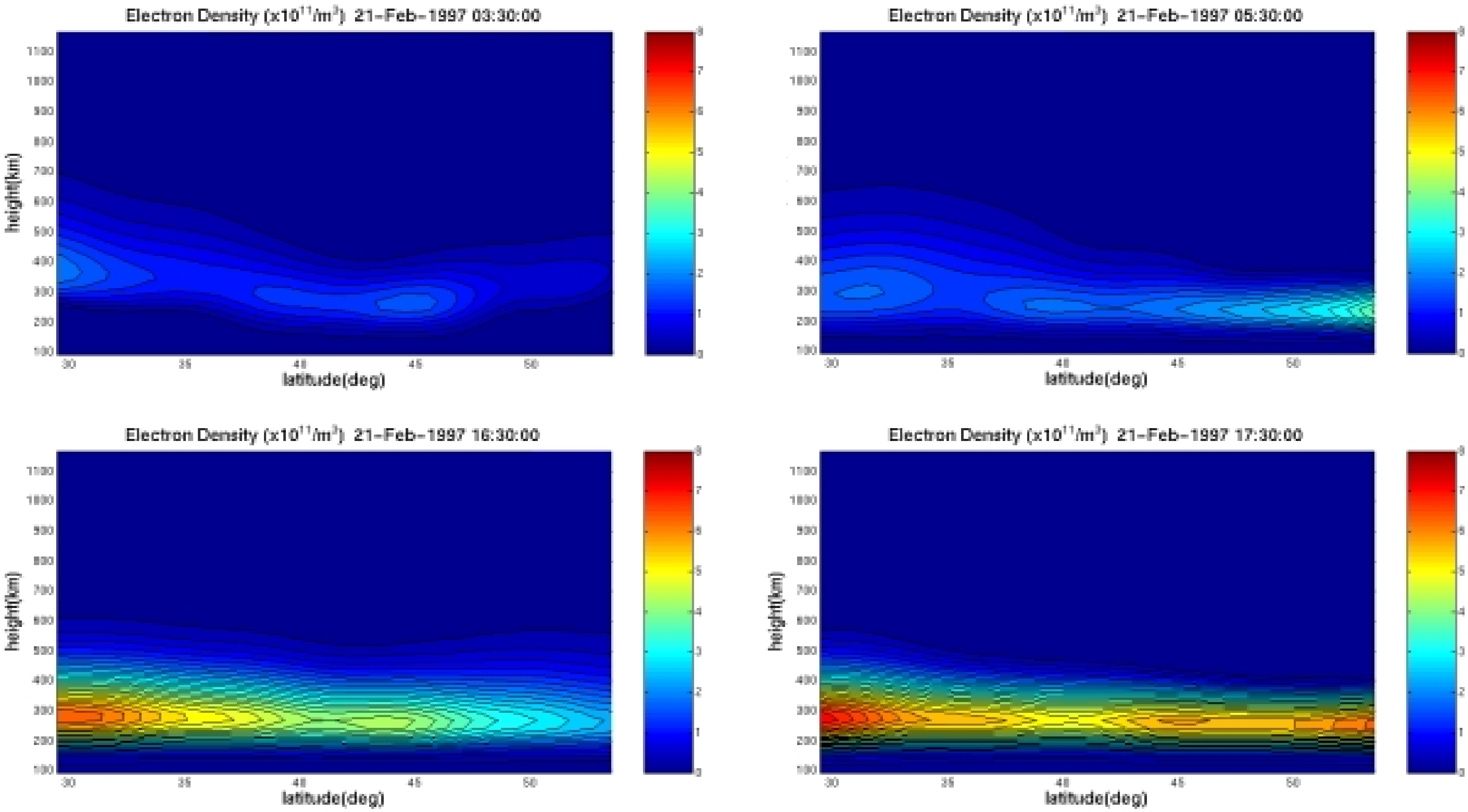

Figure 13. Cross-sections of electron concentration ($x10^{11}m^{-3}$) for 21 February 1997. The diurnal variation in peak height and scale height can be clearly seen.

5 Storm Case Study: 14th to 16th July 2000

The previous case study was carried out during a magnetically quiet period close to sunspot minimum. This second case study presents results from a storm period during sunspot maximum. During this period only ground-based IGS data was available and the network of selected ground-based receivers from North America is shown in Figure 14.

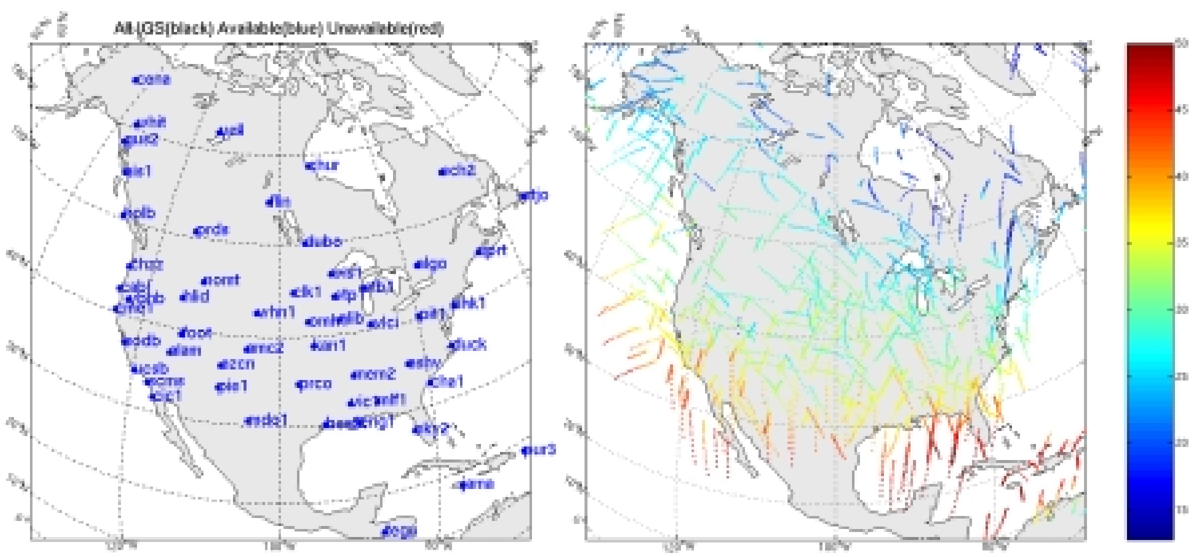

Figure 14. IGS receivers and typical shell intersection points for 00UT on 14th July 2000. Intersection points are colored according to their vertical TEC through an infinitesimal shell.

A complete set of images of the vertical TEC and electron concentration cross-sections for the period around the storm are given in the Appendix. The comparisons span a period of three days. The Kp values are shown in Table 2.

Day	**Kp**							
14th	4	3	4	4	4	6	5	4
15th	4	4	5	5	6	9	9	9
16th	8	6	5	4	4	3	3	3

Table 2. Kp values from 14th to 16th July 2000 (obtained from UK World Data Center).

Figure 15 shows the comparison between observations of NmF2 from three different ionosondes and the corresponding values from the MIDAS inversions. The diurnal trend in NmF2 is clearly apparent, with all three ionosondes showing generally good validation of the MIDAS results on the 14th July (Day 196). The nighttime comparisons on 14th and

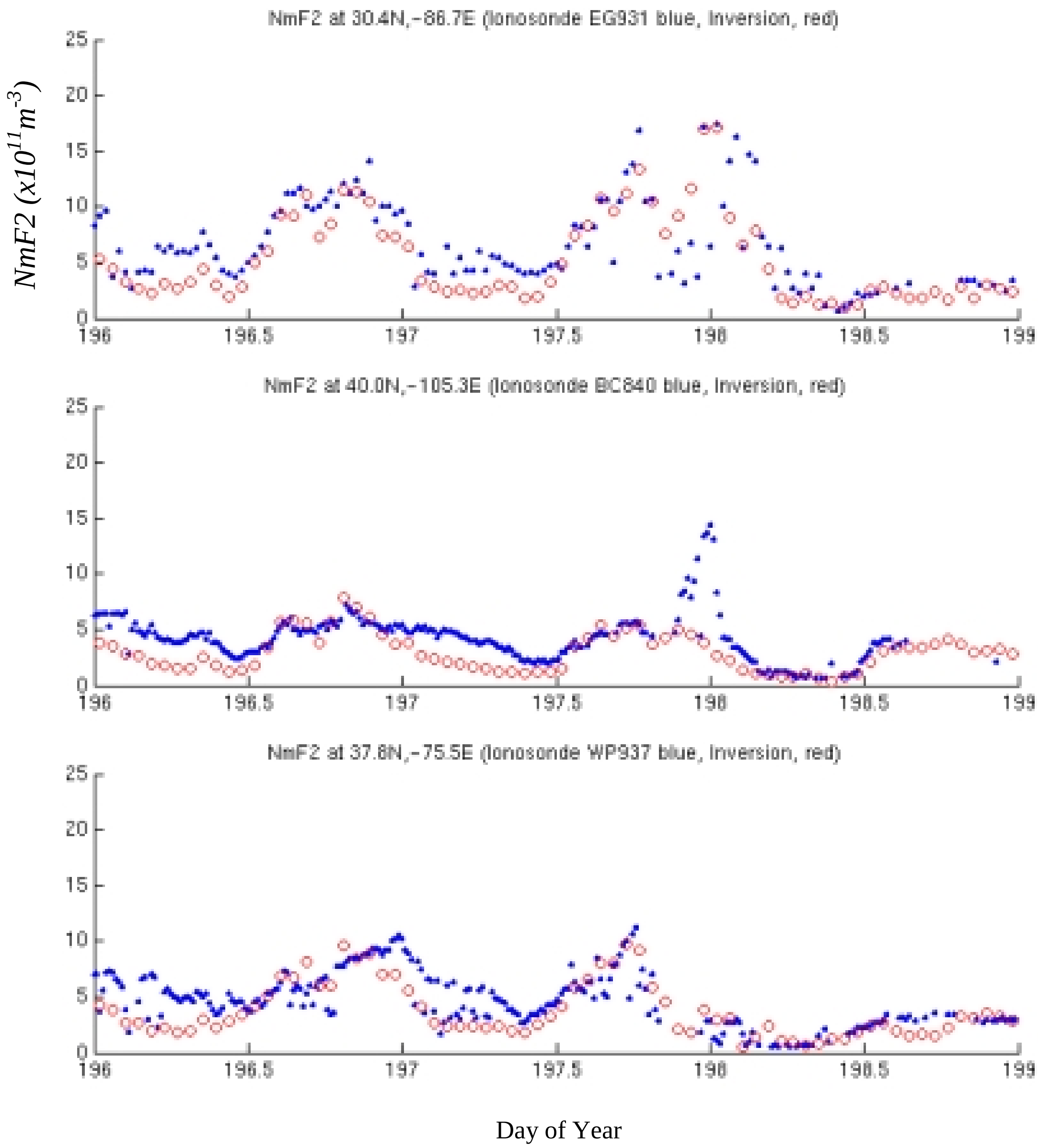

Figure 15. Comparison of NmF2 from ionosondes and inversions using ground - based GPS data from 14th July 2000 to 16th July 2000.

15th generally show an overestimation of peak electron concentration from the MIDAS inversion. This is probably a consequence of the large range of profiles required to create a sufficiently varied basis set of EOFs for these storm conditions, where the vertical profile can be very different from that found during quiet conditions. In order to stabilize the inversions with the same parameters for the full three days, it was necessary to give extensive freedom to the basis sets, with peak heights ranges extending to above 600 km. Initially it was thought that this extreme peak height in some images (towards the end on 15th July) could be an artifact caused by instability in the inversion. However, other instrumentation indicates that it is likely to be correct. Notably the sharp increases in NmF2 seen by the ionosondes on the 15th co-locate with images of the very steep wall of ionization (Figures A2 and A4). It is likely that these very high-density ionosonde soundings could be from the higher values found slightly off vertical on the ionization wall, rather than directly overhead and hence the discrepancy with the inversion values of NmF2 in the voxels above the ionosondes. It is intended that a more extensive investigation into these images of the storm effects will be undertaken.

6 Conclusions

The new technique of inversion imaging (MIDAS) has been presented, extending the established tomographic methods. The MIDAS inversions result in 3-D 'movies' rather than the static 2D slice produced by a tomographic inversion. Individual frames of the movie can then be used for spatial studies of the ionosphere and studies of the temporal changes in the ionosphere can be made with successive frames. This new work is a major and significant advance over the capabilities offered by 2-D tomography.

This report clearly shows that the MIDAS method can be applied to large-scale ionospheric inversion problems when sufficient density of observations is available. Ground-based GPS receivers are sufficiently numerous over Europe and the US to enable accurate TEC images over these regions to be generated.

There are three main results arising from this study:

1. **Thin-shell or full inversion.** It has been shown by simulation that in the presence of localized horizontal gradients such as the main trough the shell approximation provides very poor results. A full inversion offers a significant improvement in the determination of vertical TEC.
2. **Ground-based GPS data.** It is apparent that an approximate estimate of the variations in the mean height (controlled by both the peak and scale height) of the ionosphere can be resolved using ground-based data alone. A major achievement has been the stabilization of the inversion throughout the storm of July 2000, possibly the most difficult mid-latitude ionospheric condition to cope with.
3. **Radio-occultation data.** (i) Data from space-based GPS platforms in low-Earth orbit provide information that is vital for the most accurate determination of the distribution of the ionization in the vertical direction. (ii) The improvement in the results where radio-occultation data were included was significant at the edge of the

image region. This indicates that the radio occultation data would improve the imaging accuracy over data-sparse regions such as oceans.

This research has established the importance of GPS for ionospheric study, and indicates the value of the data for routine ionospheric mapping applications. In particular, the new radio occultation data adds a significant amount of information about the vertical profile and hence could prove important for HF applications. Further work should concentrate on assessing the importance of other instrumentation in the inversion. This will include an extensive evaluation of the following data:

1. Langmuir probe in-situ electron concentration measurements
2. Sea reflecting radar data.

There are currently dual-frequency GPS receivers from about 200 locations providing data to the IGS network, providing an unprecedented opportunity for ionospheric imaging. The conventional techniques to calculate vertical TEC from such data can be improved on with the MIDAS inversion. The increasing availability of LEO satellite ionospheric data in the near future will allow global ionospheric imaging, including oceans, poles and those remote regions with hostile terrain where ground-based instrumentation cannot be deployed.

7 References

Austen, J.R., S.J. Franke, C.H. Liu, and K.C. Yeh, 1986, Application of computerized tomography techniques to ionospheric research, *Proc. International Beacon Satellite Symposium*, **25**, Oulu, Finland.

Fremouw, E.J., J.A. Secan and B.M. Howe, 1992, Application of stochastic inverse theory to ionospheric tomography, *Radio Science*., **17**, 721.

Hajj, G.A. R. Ibañez-Meier, E.R. Kursinski and L.J. Romans, 1994, Imaging the ionosphere with the Global Positioning System, *Int. J. Imag. Syst. Technol.*, **5**, 174.

8 Acknowledgements

International GPS Service for the ground-based GPS data.

UCAR, USA for the GPS/MET LEO radio-occultation data.

The MIDAS inversion program (© University of Bath) was developed under a grant awarded by the UK Engineering and Physical Sciences Research Council.

9 Appendix

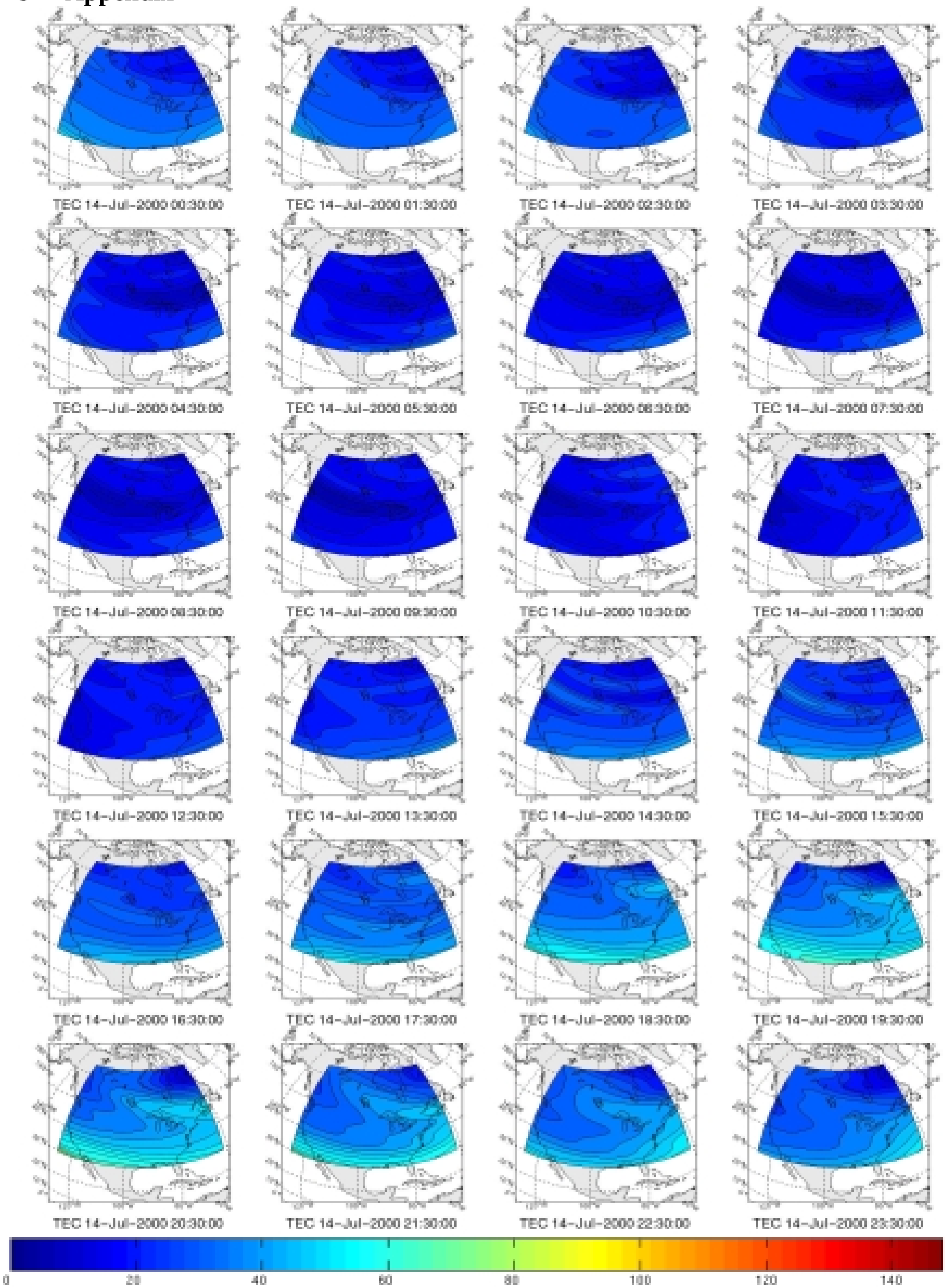

Figure A1. Vertical total electron content (TECU) on 14th July 2000.

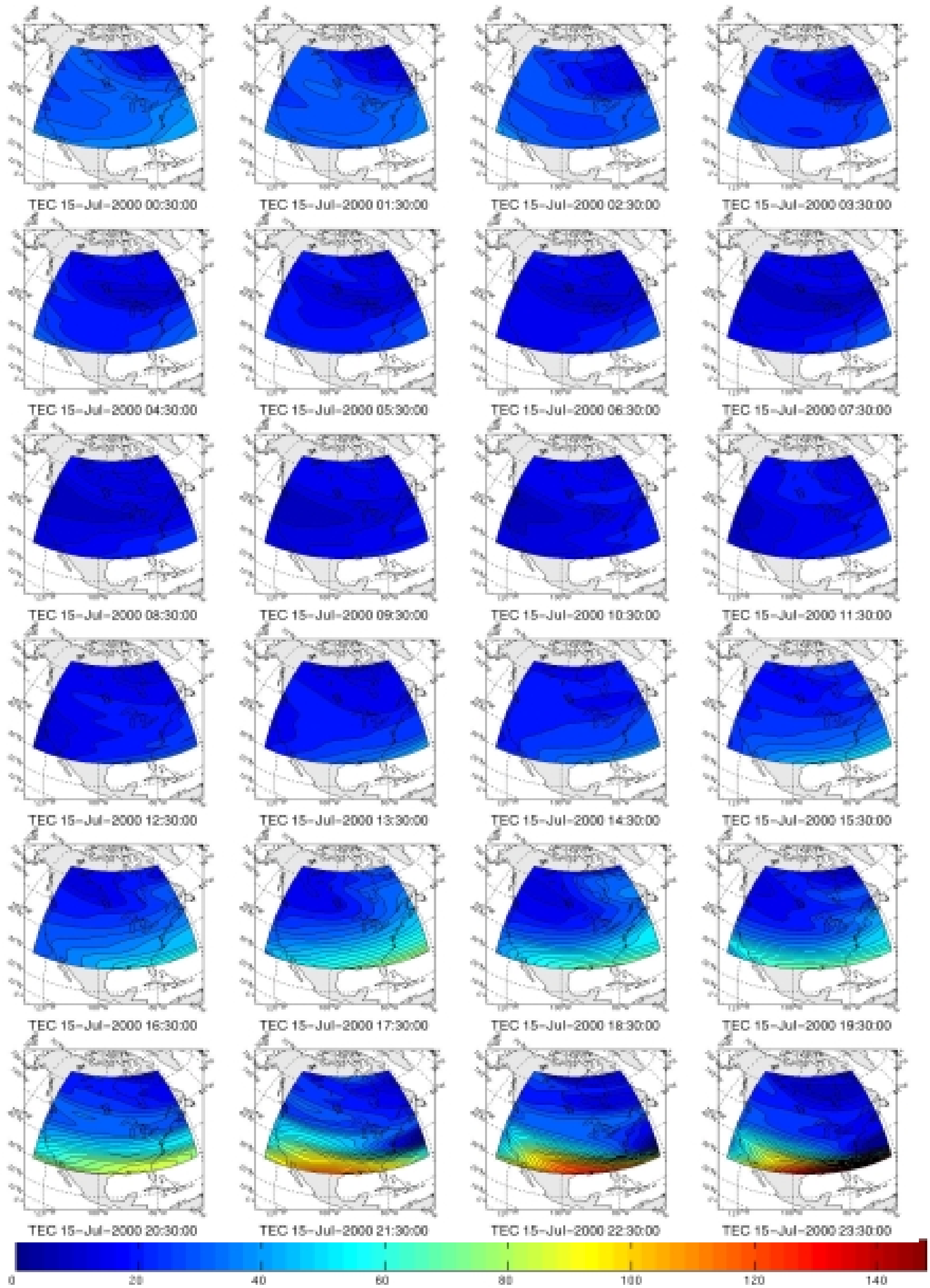

Figure A2. Vertical total electron content (TECU) on 15th July 2000.

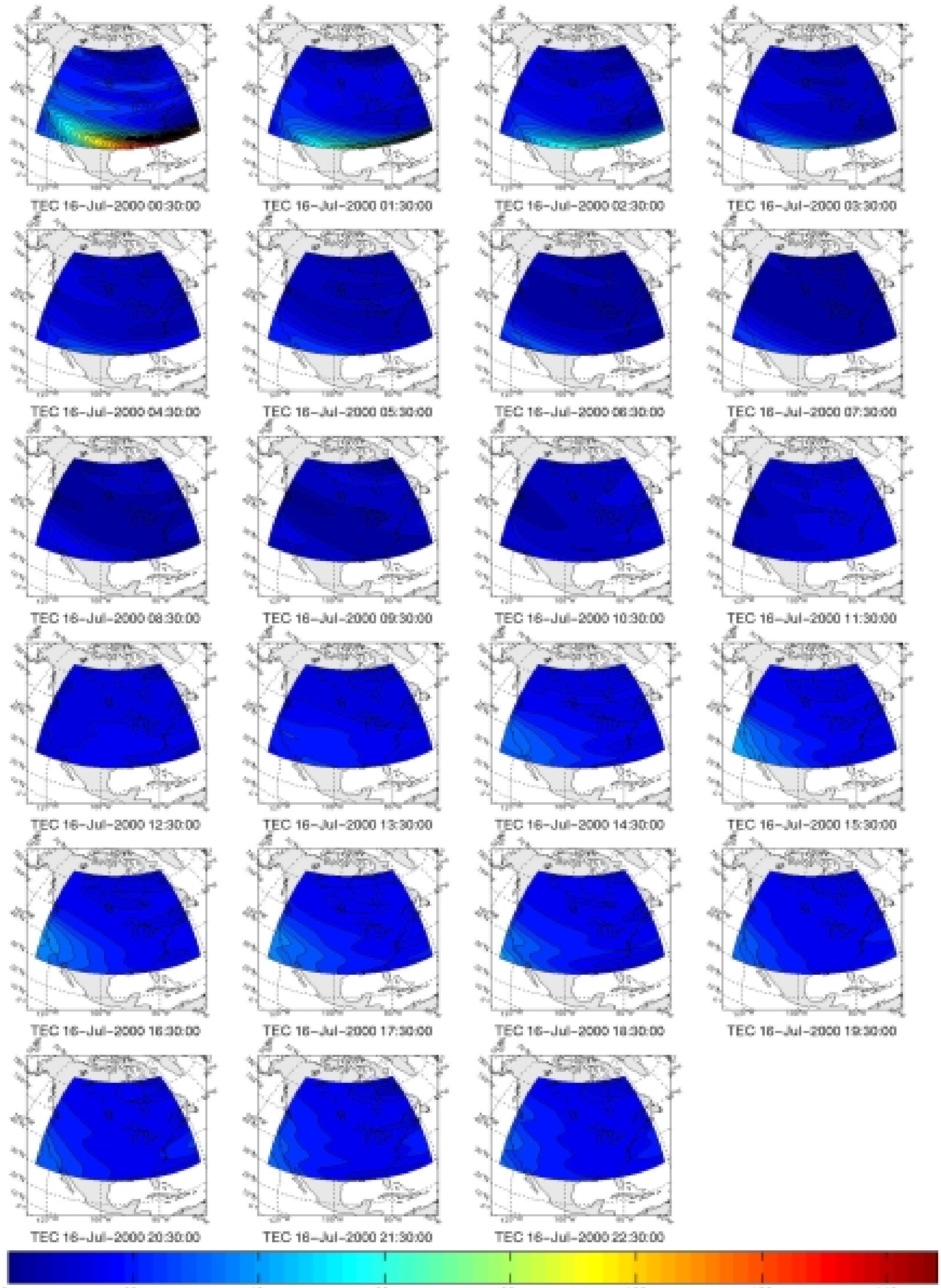

Figure A3. Vertical total electron content (TECU) on 16th July 2000.

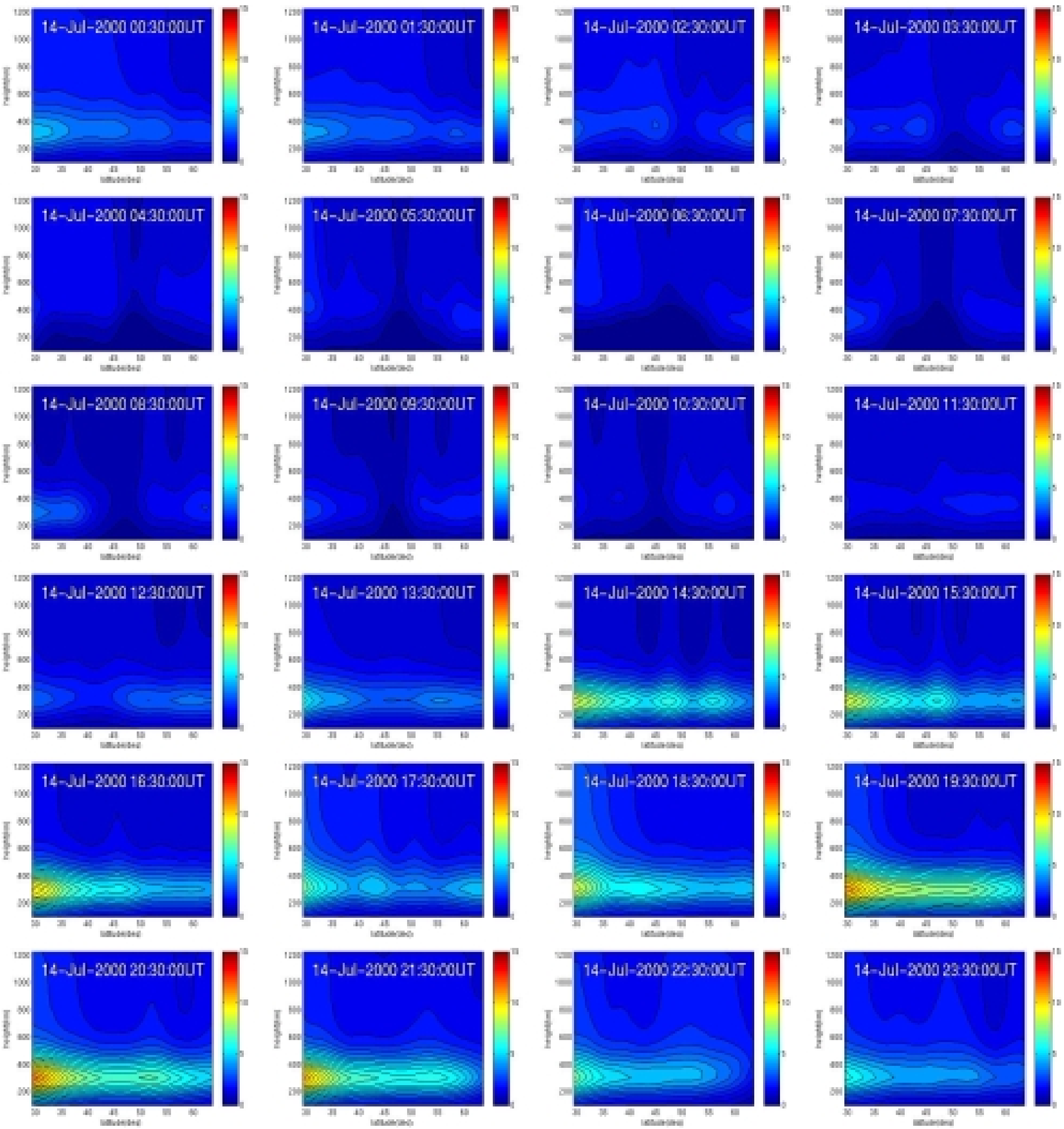

Figure A4. Electron concentration cross-section ($x10^{11}/m^3$) at 98°W on 14th July 2000.

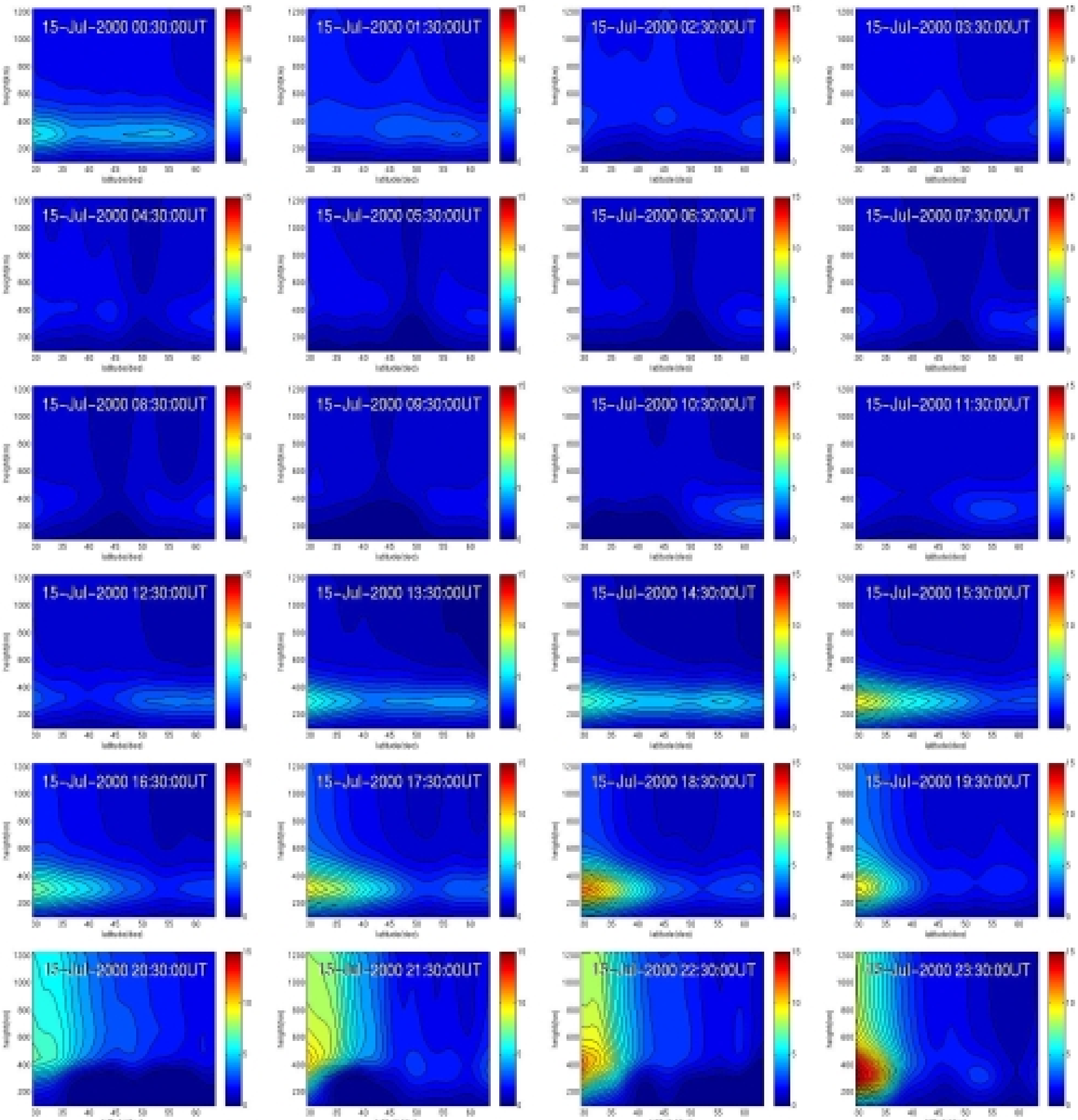

Figure A5. Electron concentration cross-section ($x10^{11}/m^3$) at 98°W on 15th July 2000.

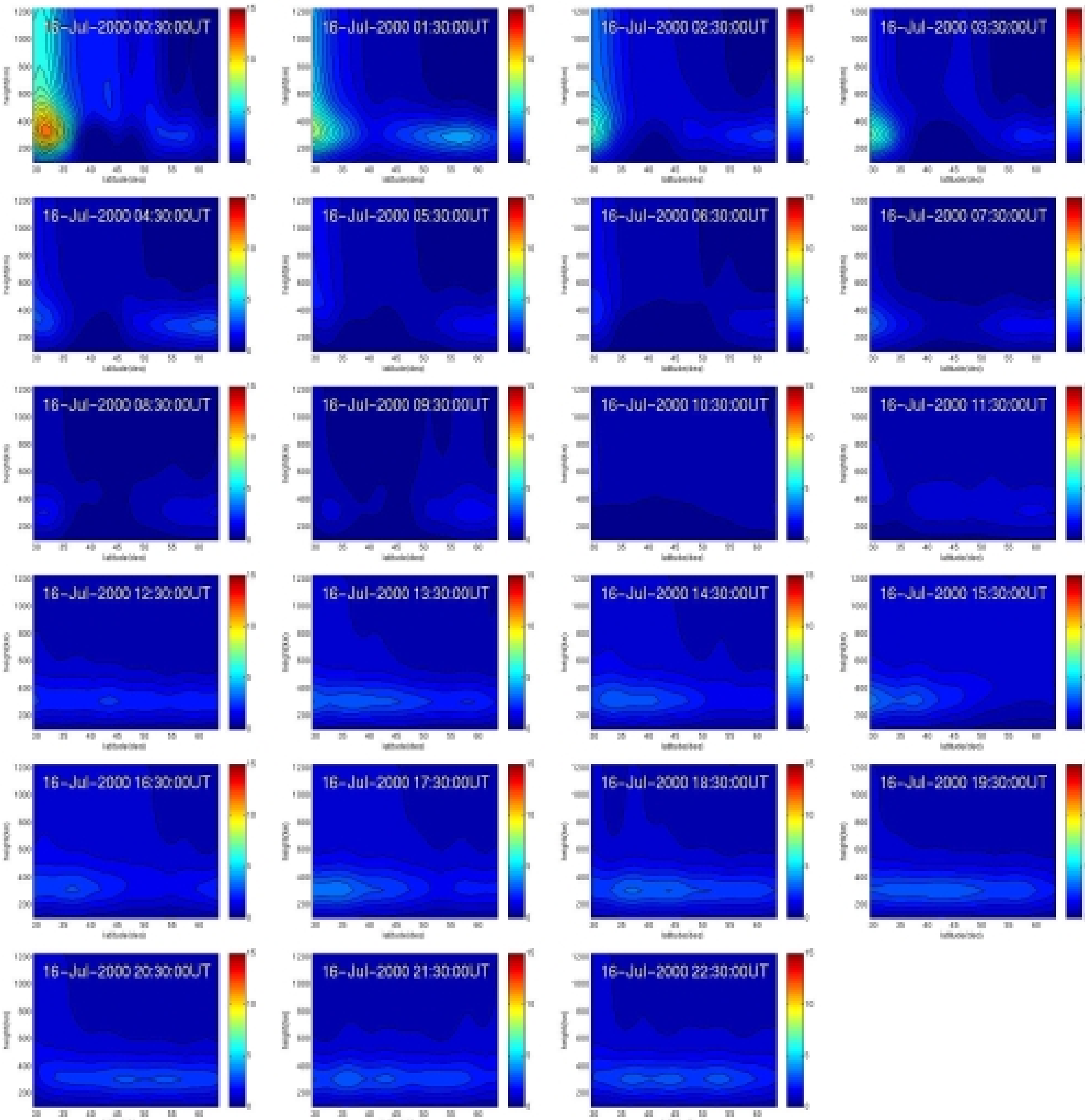

Figure A6. Electron concentration cross-sections (x10^{11} m^{-3}) at 98°W on 16th July 2000.